

Preparation and melting of amorphous silicon by molecular-dynamics simulations

W. D. Luedtke and Uzi Landman

School of Physics, Georgia Institute of Technology, Atlanta, Georgia 30332

(Received 8 September 1987)

Molecular-dynamics simulations of amorphous silicon are described, using the two- and three-body interaction potentials constructed by Stillinger and Weber. The amorphous-material preparation procedure is described and the structural and dynamical properties of the amorphous phase are simulated and analyzed. The characteristics of the simulated amorphous phase compare favorably with experimental data and with structural models. Upon rapid heating, the amorphous sample melts via a first-order transition at a temperature of 230 K below the melting temperature of the crystalline material with a latent heat approximately equal to 0.2–0.4 of the latent heat of the crystalline-liquid transition. The nature of the transition and the magnitude of the latent heat maintain, but shift to a lower temperature, for melting of fully relaxed amorphous configurations at elevated temperatures.

I. INTRODUCTION

Amorphous materials represent a large area of endeavor in material science on both the basic and technological frontiers.^{1–3} Particularly challenging are the structural properties of these materials (amorphous semiconductors, in particular) which have been the subject of numerous experimental and theoretical studies^{1–3} and controversy. The difficulty in studying matter in the amorphous state originates from the lack of periodicity which hinders the use of conventional condensed-matter structural determination and modeling methods. Consequently, in attempting to define this state of matter it is often easier to state what it is not than to provide a precise definition. A main issue in studies of amorphous semiconductors (and other materials) is the structural characterization of these systems. Therefore, efforts have focused on analysis and modeling of the structure of elemental amorphous systems where only positional disorder is present. Early suggestions⁴ that the amorphous state of Si and Ge is microcrystalline have been shown to be inconclusive,⁵ leading to the development of various models^{6–9} in which disordered structures are hand built or computer generated according to well-defined algorithms. Among these, we note the continuous random network (CRN) based models⁶ and in particular a variant of it, proposed by Wooten, Winer, and Weaire⁹ (WWW), in which the amorphous structure of a tetrahedrally bonded material is generated from the crystalline state by a series of selected atomic rearrangements coupled with relaxation and energy optimization via a procedure which resembles simulated annealing.¹⁰

Although the above structural models aid the elucidation and interpretation of data, alternative descriptions in terms of interatomic potentials are required in order to investigate the response of materials to changes in external physical conditions and the dynamics and mechanisms of phase transformations (such as melting, crystallization, and amorphization), and to allow molecular-dynamics (MD) simulations of material processes. While

a variety of models for many materials have been constructed and employed for some time,¹¹ the formulation and implementation of interaction potentials which provide an adequate description of covalently bonded materials (semiconductors, in particular) is only a recent development.^{12–15} The potential constructed by Stillinger and Weber (SW) which includes two- and three-body interactions has been used recently in several MD studies of bulk^{16–18} and surface phenomena¹⁹ and in studies of equilibrium^{20,21} and nonequilibrium²² solid-melt interfaces of silicon. In addition, a reparametrized SW potential has been employed in investigations of Ge.¹⁷ While the SW potential which was parameterized¹² on the basis of solid and liquid phase data for Si yields an adequate description of these aggregation states, it has been reported^{16,17} that it fails to describe the amorphous state and it has been concluded that the SW potential or a reparameterization of it, cannot handle these three different phases simultaneously. It appears¹⁶ that this potential produces a range of degenerate disordered structures, and that the difference of the configurational entropies of the low-temperature liquid and amorphous phases is in error resulting in a too small value of the heat of fusion for the liquid to amorphous transition. Consequently, studies of phenomena which may involve a liquid-to-amorphous transition could be handicapped by the inability to quench a SW liquid directly into an amorphous structure. On the other hand, in many instances the phenomena under study allows one to start from the amorphous state, without passing through the liquid-to-amorphous transition region. For such cases (which include systematic studies of the amorphous phase under various conditions, the properties of the amorphous-crystalline interfaces and processes which may involve amorphous-to-liquid transition) we seek a method of *preparing* the system in the *correct* amorphous state. Furthermore, we require that the so prepared material will maintain the correct characteristics of the amorphous phase, including those in the amorphous-to-liquid transition region, when described via the SW potential. In Sec. II we describe a

procedure which we have developed for the preparation of amorphous silicon, using the SW interaction potentials. We then characterize the amorphous phase, which we prepared, structurally and dynamically yielding results which are in good agreement with experiments. The first-order melting transition of the amorphous to the liquid phase is discussed in Sec. III.

II. PREPARATION PROCEDURE AND CHARACTERIZATION OF AMORPHOUS SILICON

We describe in this section a method for preparing amorphous Si whose structural and thermodynamic properties are in good agreement with available data, and which allows the employment of the SW potential over a wide range of external conditions. A basic element of the method is the observation that the three-body term in the potential energy is responsible for the directional character of the structure. Since the original parametrization of the SW potential results in a failure to assume the correct amorphous structure upon cooling^{16,17} we redirect the path which the system traverses in the multidimensional configurational space by enhancing the tendency toward tetrahedral angles in the initial stage of the preparation procedure. This is achieved by increasing the magnitude of the coefficient multiplying the three-body potential term by 50% during the cooling process. Once the system has reached the amorphous basin the original SW potential is restored and the system evolves toward the correct amorphous state. A similar procedure was attempted by Broughton and Li.¹⁶ We note that our preparation procedure is in the spirit²³ of experimental procedures for the preparation of amorphous solids via melt quenching, vapor condensation, electrodeposition, ion sputtering, or intense irradiation. In all these methods the material is brought through a penultimate state which has a higher free energy than the amorphous state. The material is then put into the amorphous by bypassing crystallization.

In our constant-pressure MD simulations Newton's equations of motion are integrated using Gear's fifth-order predictor-corrector algorithm for a system of 588 particles contained in a periodically replicated calculational cell which possess full dynamical freedom to change shape and volume according to the ansatz Lagrangian method of Parrinello and Rahman.^{24,22} Using an integration time step, $\Delta t = 1.15 \times 10^{-3}$ psec, and interaction lists which are updated every 8 Δt , energy conservation to at least six significant figures is achieved over a time span of $10^4 \Delta t$. In the following we use reduced units in which energy and temperature are expressed in units of $\epsilon = 50$ kcal/mol (to convert to T in K multiply the reduced temperature by 2.5173×10^4) and the unit of length is $\sigma = 2.0951$ Å. The time unit (t.u.) is $\sigma(m/\epsilon)^{1/2} = 7.66 \times 10^{-14}$ sec. The parametrization of the potential is as given by SW,¹² i.e.,

$$V_2(r_{ij}) = A(Br_{ij}^{-P} - 1)g_\gamma(r_{ij}), \quad (1a)$$

$$V_3(r_i, r_j, r_k) = v_{jik} + v_{ijk} + v_{ikj}, \quad (1b)$$

$$v_{jik} = \lambda g_\gamma(r_{ij})g_\gamma(r_{ik})(\cos\theta_{jik} + \frac{1}{3})^2, \quad (1c)$$

where V_2 and V_3 are the two- and three-body potentials, respectively. r_{ij} is the distance between atoms i and j , and $g_\gamma(r) = \exp[\gamma/(r-a)]$ for $r < a$ and vanishes for $r \geq a$. The values of the parameters of the potential are $A = 7.044556277$, $B = 0.6022245584$, $P = 4$, $a = 1.8$, $\lambda = 21$, $\beta = 1$, and $\gamma = 1.2$. The melting temperature of the SW silicon crystal is²⁰ $T_{cl} = 0.0662 \pm 0.0016$ (1665 K) in good agreement with the experimental value, 1683 K, and the per-particle latent heat ΔH_{cl} is²⁰⁻²² 0.15ϵ (31.4 kJ/mol) compared to the experimental value of 50.7 kJ/mol. The external pressure in all our simulations is $P_{ext} = 0$.

Our preparation procedure consists of the following steps.

(1) We start from a SW liquid which we equilibrated at $T = 0.2$ for $6000\Delta t$, keeping the shape (but not the volume) of the calculational cell constant. This step serves to "mix" the system at a high temperature.

(2) Keeping the cell shape fixed, the coefficient λ of the three-body potential is increased from the SW value by 50% in order to enhance tetrahedral coordination,²⁵ and the system is run for an additional $6000\Delta t$.

(3) The temperature is lowered to $T = 0.067$ (via scaling of the particle's velocities) over $2000\Delta t$, and then the system freely evolves with no further temperature control, for $6000\Delta t$. Subsequently, the system runs for an additional $6000\Delta t$ but with full dynamics of the calculational cell (shape and volume). During the last $12000\Delta t$ the temperature rises to ~ 0.084 , the density increases from $\sim 0.408\sigma^{-3}$ to $0.4155\sigma^{-3}$, and the three-body potential drops. At the temperature of 0.084 the particle diffusion is about an order-of-magnitude smaller than that for the SW liquid at this high temperature.

(4) Starting from $T = 0.084$ we cool the system over a time span of $48000\Delta t$ by removing an energy of 0.0014ϵ per particle (i.e., between energy extractions the system evolves for $250\Delta t$ every $250\Delta t$). At the end of this stage the temperature drops to 0.014 (room temperature in the reduced units is ~ 0.012). It is of interest to note that at $T \leq 0.075$ the diffusion constant is exceedingly small which, coupled with a change of slope in the total energy versus temperature curve, perhaps indicate a glass transition of the $\lambda = 31$ system. At the end of this stage the density of the system is $0.43\sigma^{-3}$ (much lower than the correct amorphous density of silicon).

(5) The coefficient λ is decreased back to the SW value over a time span of $2000\Delta t$. Properties of the system change rapidly during this period following the change in λ (see the initial period in the temperature, density and potential energy plots versus time shown in Fig. 1).

(6) The system evolves freely for $40000\Delta t$, resulting in a relaxed amorphous material. The properties of the system are shown in Fig. 1 ($\rho \cong 0.448\sigma^{-3}$, $T = 0.0143$). The density of a crystalline SW silicon at this temperature is $0.455\sigma^{-3}$. Thus in keeping with experimental data the density of our amorphous sample is $\sim 1.5\%$ below that of the crystalline one, and is slightly lower than the density of the continuous random network model of WWW.^{9,16} Note also that the density of our amorphous material is much lower than the "indirect amorphous" density of Broughton and Li,¹⁶ which is higher than the crystalline

density.

Structural characterization of the material is provided via the radial pair-distribution functions (RDF) $g(r)$ (Fig. 2) and the three-body correlation function $g_3(\cos\theta)$ (Fig. 3). In addition to the $g(r)$ and $g_3(\cos\theta)$ of the amorphous material (*a*) we display in Figs. 2 and 3 the pair and triplet distributions for the room-temperature SW solid (*c*), for a SW liquid (*l*) at the melting point, and for a SW glass (*g*) which was prepared following the same

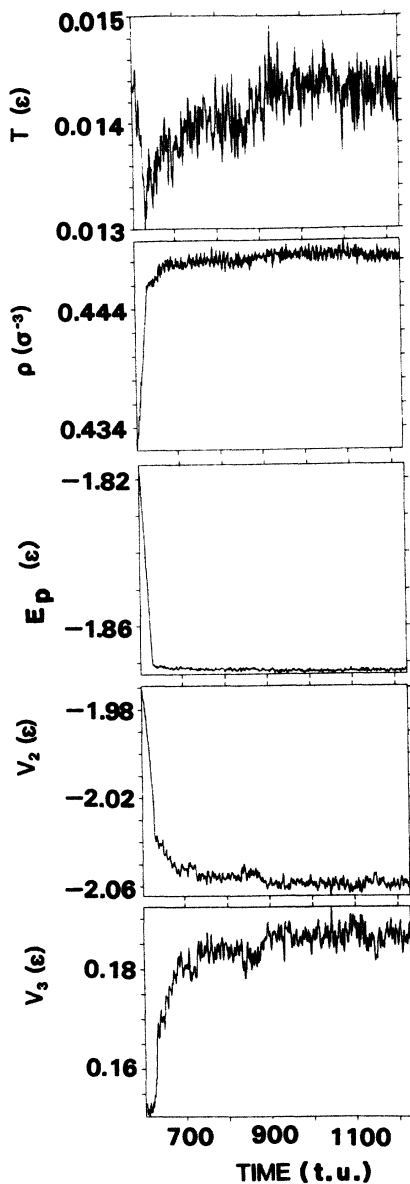


FIG. 1. Time evolution (in units of SW t.u. = 7.66×10^{-14} sec) of the temperature T , density ρ , the per-particle potential energy E_p , and of the individual two- and three-body contributions V_2 and V_3 , respectively, during stage (5) of the preparation procedure. The sharp variations during the first 2000 Δt occur as a result of switching the parameter λ of the three-body term in the potential from 31 to the original SW value (21). The relaxation of the material at later times is evident. Energies and temperature in units of $\epsilon = 50$ kcal/mol and density in units of σ^{-3} ($\sigma = 2.0951 \text{ \AA}$).

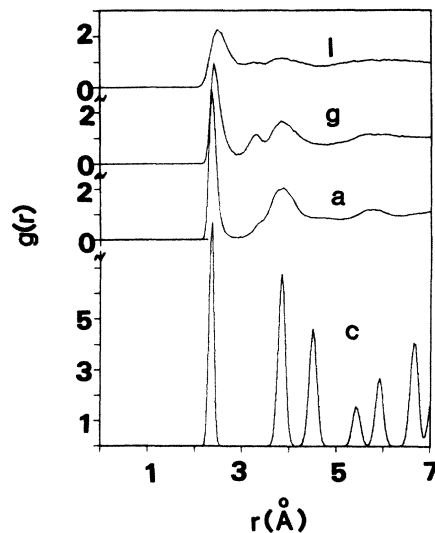


FIG. 2. Radial pair distribution functions, $g(r)$, for SW Si crystal (*c*), amorphous (*a*), and glass (*g*) at $T \approx 0.014$, and for a SW liquid (*l*) at the crystal melting point $T_{c1} = 0.0662$. Note the differences between the peak locations and peak heights for the different phases, and in particular the almost disappearance of the second peak in comparing the glass and amorphous $g(r)$. Distance in units of \AA .

procedure as described in steps 1–6, but with no change in the coefficient of the three-body potential. $g_3(\cos\theta)$ gives the probability distribution of $\cos\theta$ for the angle $\theta = \theta_{ijk}$ between a triplet of particles i, j, k whose bond lengths (r_{ji} and r_{jk}) about the angle which they subtend (with particle j at the vertex) are both less than the first minimum in the pair-distribution function $g(r)$. In comparing the RDF's for the crystalline and amorphous solids we observe that in agreement with experiment,²⁶ the first and second peaks appear in both RDF's, though broadened in the amorphous system, as well as the fourth

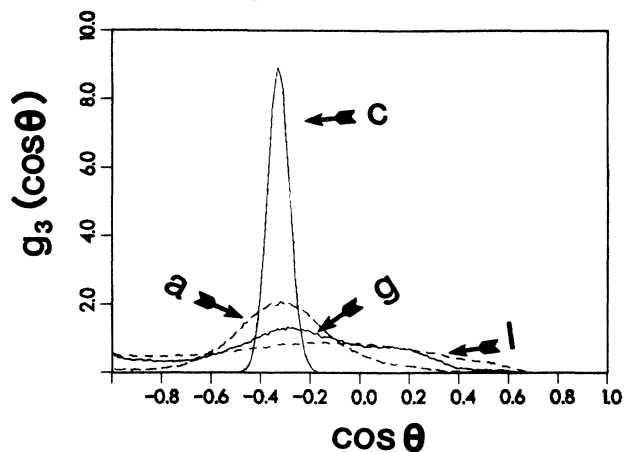


FIG. 3. Three-body correlation functions, $g_3(\cos\theta)$, for SW crystal (*c*), amorphous (*a*), and glass (*g*) at $T \approx 0.014$, and for a SW liquid (*l*) at the crystal melting point $T_{c1} = 0.0662$. Note the broadening and shift in the maximum upon going from the crystal to the liquid. Also note the shoulder in the glass distribution function, (the values of the average angles and rms deviations are given in Table I).

TABLE I. Fraction of atoms with given coordination, average bonding angle θ , and its standard deviation and densities at the following temperatures: room temperature for the amorphous, glassy, and crystalline phases, and T_m for the liquid. The SW silicon potential (Ref. 12) was used in the calculations. Density in units of σ^{-3} ($\sigma=2.0951 \text{ \AA}$).

Coordination	Amorphous	Glass	Crystal	Liquid
3	0.005	0.002	0	0.023
4	0.878	0.410	1	0.294
5	0.115	0.522	0	0.477
6	0.003	0.066	0	0.185
7	0	0.001	0	0.021
θ	108.3 ± 14.7	106.6 ± 22.6	109.4 ± 2.7	103.9 ± 26.8
ρ	0.448	0.489	0.455	0.482

and fifth peaks which in the amorphous case are broadened and merged into a single peak. Significantly, the third, prominent, peak in the crystalline RDF is missing in the amorphous structure as observed experimentally²⁶ and in the WWW model.^{9,16} Our results agree with the experimental ones and those of the WWW model in both peak locations and height. We also note the absence of the third crystalline peak in the RDF for the SW glass. The RDF's for the amorphous and glass, however, differ in peak heights and the existence of a pronounced bump on the lower distance side of the second peak in the glass RDF which is a characteristic of glass structure.

Insight into the type and degree of short-range order in the system is provided by the angular, triplet, distribution functions shown in Fig. 3. We observe first that the crystalline $(c)g_3$ is sharply peaked about the tetrahedral angle. For the amorphous phase, the peak is still about the tetrahedral angle but is significantly broadened with a rms angle deviation of 14.7° (see Table I). These characteristics are in accord with experiment⁵ and with the WWW relaxed CRN model.^{9,16} In the glass (*g*) we observe a slight shift of the maximum position to a lower angle, further broadening and the development of a shoulder at about 85° .

Further characterization of the structure is given by the fraction of atoms with a given nearest-neighbor coordination, i.e., to a distance of the first minimum in $g(r)$. The data for the amorphous, glass, liquid, and crystalline phases is given in Table I. Our results for the amorphous phase are in close agreement with the WWW amorphous model¹⁶ exhibiting the dominance of fourfold coordination and the existence of fivefold coordination. In the glass state the fourfold and fivefold coordination become comparable. In the liquid fivefold coordination is dominant accompanied by mainly four and sixfold coordination.

A dynamical characterization of condensed-matter systems is provided by the density of vibrational states, $D(\omega)$ spectra. In Fig. 4 we show the density of states for the amorphous, crystalline SW glass, and liquid [$D(\omega)$ is normalized so that the integral under the curve is unity]. These were obtained by Fourier transforming the particle velocity autocorrelation function. First we note the close similarity between $D(\omega)$ for our prepared amorphous

material and that calculated by Broughton and Li¹⁶ using the WWW model coordinates.⁹ There is a significant increase in the density of low-frequency modes in the amorphous and glassy states as compared to the crystalline spectrum. The diffusion constant in the liquid phase can be determined from the finite value of $D(\omega)$ at $\omega=0$.

III. THE AMORPHOUS-TO-LIQUID TRANSITION

The melting of amorphous Si (and Ge) has been a subject of great interest, motivated by studies of rapid melt-

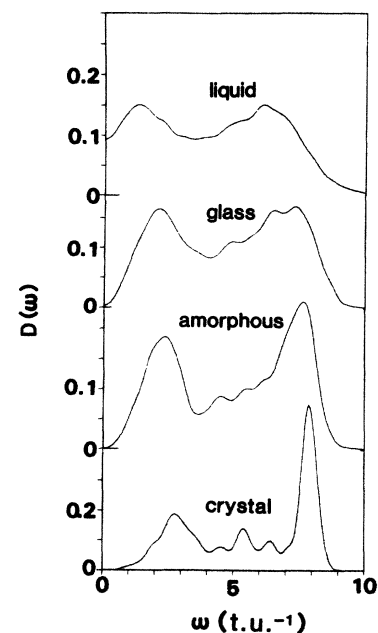


FIG. 4. Density of states, $D(\omega)$, calculated as Fourier transforms of the velocity autocorrelation functions for SW crystal, amorphous, and glass at $T \approx 0.014$, and for a SW liquid at $T_{cl} = 0.0662$. The frequency, ω , is in units of the inverse SW time unit (t.u.). $D(\omega)$ is normalized such that the integral over ω is unity. A Gaussian apodization was used in order to take account of the finite span of time records. Note the growth of the population of the low frequencies for the amorphous, glass, and liquid states as compared to the crystal. The finite value for the liquid $D(\omega)$ for $\omega=0$ is proportional to the liquid diffusion constant.

ing and solidification (known as laser annealing²⁷). The observation that the amorphous materials have higher free energies than the crystalline forms led to the proposal^{28,29} that the amorphous phase melts via a first-order transition at a discrete temperature (T_{al}) that is lower than the melting temperature of the crystalline material (T_{cl}). This led to a number of experimental investigations of the thermodynamic properties of the amorphous-to-liquid transition.^{30,31} Current estimates³⁰ place T_{al} in the range of 200–300 K below T_{cl} , with a latent heat ΔH_{al} for the amorphous-to-liquid transition³¹ being 34.3 ± 4.2 kJ/mol as compared to the latent heat for the crystal-to-liquid transition, $\Delta H_{cl} = 50.7$ kJ/mol.

Having obtained amorphous silicon described by the SW potential, we turn now to an investigation of the melting transition of this material. First we describe the behavior of the system when the heating rate is the same as the rate of heat extraction which we employed in preparing the amorphous sample. Starting from the amorphous sample as $T = 0.0143$ the system was heated by adding energy (via scaling of particle velocities) at a rate of 0.0014ϵ per particle, every $250\Delta t$, over a time span of $32000\Delta t$. The temperature of the system versus time during this run is shown in Fig. 5 exhibiting at first a linear increase which is interrupted at ~ 230 t.u. (where melting initiates) and resumes at ~ 320 t.u. In Fig. 6 we show the total energy (per particle) and density of the system versus temperature. The melting transition is evident from these time plots. We note that the transition is rather abrupt (resulting in a discontinuity in the specific heat), with some evidence for a pretransitional, more gradual, stage. The variation of the potential energies and of

$$R^2(t) = \frac{1}{N} \sum_{i=1}^N [\mathbf{r}_i(t) - \mathbf{r}_i(0)]^2,$$

are shown in Fig. 7. The latter quantity, provides a measure of the system mobility in the N -dimensional configurational space [at equilibrium the slope of a linear relationship between $R^2(t)$ and t is proportional to the diffusion constant]. All these quantities exhibit abrupt changes at the amorphous-to-liquid transition, from amorphous-to-liquid values. In particular, note the loss of tetrahedral order upon melting evidenced by the sharp increases in the V_3 plot (the slow variation prior to the transition is due to an increase in thermal vibrations upon heating of the amorphous material).

From Fig. 6 we determine that the melting temperature of the amorphous phase for this fast heating rate is $T_{al} = 0.057$ (1435 K), i.e., 230 K below T_{cl} (the melting temperature of the crystalline material) in excellent agreement with the experimental values.³⁰ The latent heat ΔH_{al} of the transition is estimated as 0.03 – 0.06ϵ per particle (6.28σ – 12.56 kJ/mol) as compared to the value of 0.15ϵ (31.4 kJ/mol) for the SW crystalline to liquid, ΔH_{cl} , transition. In other words, $\Delta H_{al}/\Delta H_{cl} = 0.2$ – 0.4 (as compared to the experimental estimate^{30,31} of ~ 0.67). The upper bound of our estimate is obtained by judiciously taking the difference in the total energy (Fig. 6) between $T = 0.057$ and the start of the break in slope at $T = 0.048$. It should be remarked that the initial gradual change starting at 0.048 may be related to the nature of

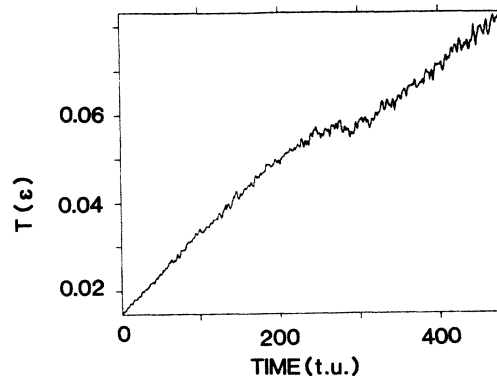


FIG. 5. Time development of the system temperature T as energy is pumped into the system starting from the relaxed SW amorphous phase at $T = 0.014$. Note the break in the curve at $t \approx 240$ t.u. signifying the initiation of a phase transformation. Time is in units of the SW t.u. and temperature in units of ϵ .

our prepared amorphous Si, and may be affected upon further refinement of the preparation procedure. Furthermore it may indicate an inherent property of SW silicon since upon heating of a SW silicon glass (see discussion above) we observed a discontinuity in the slope of the total energy versus temperature, at about the same temperature (see Fig. 8).

In order to investigate the dependence of the system characteristics upon the rate of heating we have equilibrated the system (with no temperature control) for long periods of time at several points along the heating curve (see Fig. 6). At each of these points the material relaxes

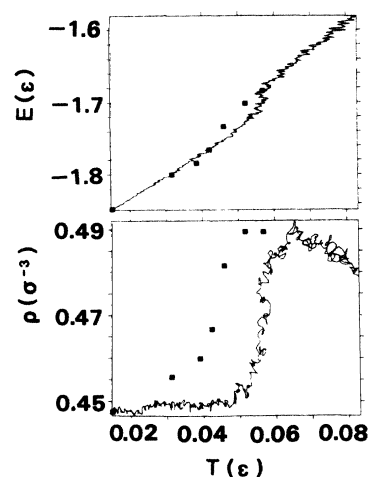


FIG. 6. The total energy per particle E and density ρ of the system vs temperature for the time period given in Fig. 5. The break in the caloric curve (E vs T) corresponds to a first-order melting transition of the amorphous material. The transition is accompanied by a sharp increase in density. The “wiggly” appearance of the density plot is due to fluctuations of the temperature in time (see Fig. 5). Energies and temperature in units of ϵ . Values obtained by fully relaxing the system at the corresponding temperatures are represented by solid dots. Note that these points trace a line similar, but shifted, compared to that obtained by rapid heating.

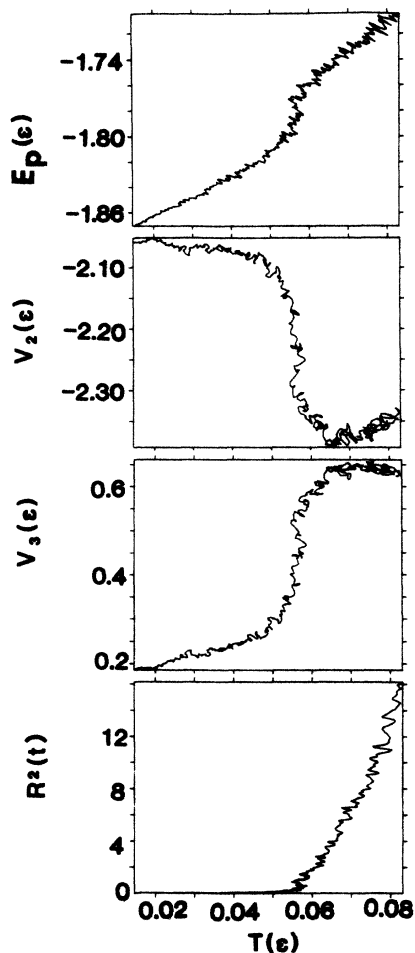


FIG. 7. Per-particle potential energy E_p and the two- and three-body contributions, V_2 and V_3 , vs temperature for the time span shown in Fig. 5. Note the sharp variation in V_3 upon melting of the amorphous phase, indicating the loss of tetrahedral order. At the bottom the function $R^2(t)$, in units of σ^2 , is shown vs temperature. As evident, no particle transport occurs in the amorphous phase until the phase transformation initiates.

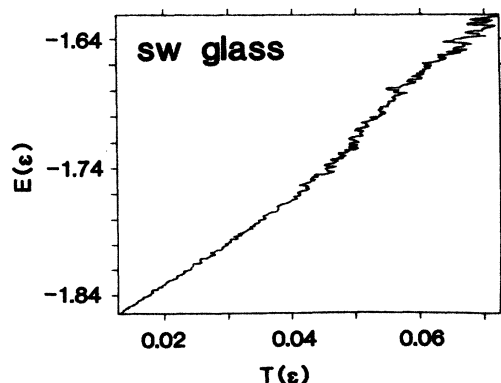


FIG. 8. The total energy per particle vs temperature during the heating of a SW silicon glass prepared as described in the text. Note the change in slope $T \approx 0.048$ which coincides with the temperature at which changes start to occur upon heating the SW amorphous silicon.

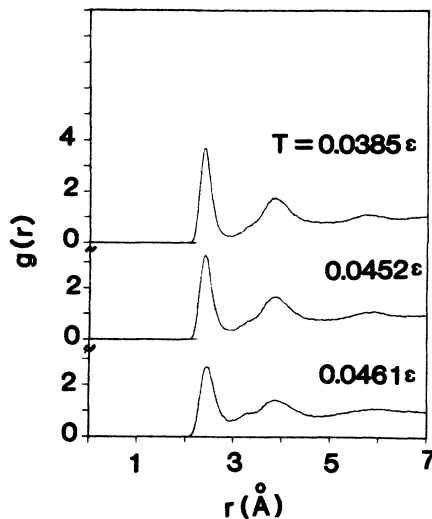


FIG. 9. Radial pair distributions $g(r)$ for the SW amorphous material fully relaxed at the denoted temperatures. Compare to the amorphous and liquid $g(r)$'s given in Fig. 2. Distance in units of \AA .

freely from its initial state to the values denoted by the points in Fig. 6. The rate at which the system relaxes decreases (necessitating very long MD runs) with the initial temperature of the system. We note that both the energy, E , and density, ρ , versus temperature curves produced in this manner show a similar behavior to those obtained via the fast heating rate, but are shifted. The radial pair-distribution functions for three points along these curves (i.e., at $T=0.0385$, 0.0425 , and 0.046) are shown in Fig. 9. Comparison between these $g(r)$'s and the radial pair distributions for the liquid and amorphous states shown in Fig. 2 reveals that at the lower temperature an amorphous material maintains. At the intermediate temperature a shift from amorphous to liquid characteristics is observed, and at the higher temperature a $g(r)$ close to that of the liquid is found. Further characterization of the relaxed configurations of the material at these three temperatures is given in Table II where fractional coordi-

TABLE II. Fraction of atoms with given coordination, average bonding angle θ , and its standard deviation and densities for relaxed configurations of the amorphous material at three temperatures. The system was run for $74\,000\Delta t$, $96\,000\Delta t$, and $30\,000\Delta t$ in order of increasing temperature. The SW silicon potential (Ref. 12) was used in the calculations. Density in units of σ^{-3} ($\sigma=2.0951\text{\AA}$).

Coordination	$T=0.0385$	$T=0.0425$	$T=0.0461$
3	0.005	0.007	0.010
4	0.675	0.590	0.387
5	0.296	0.356	0.480
6	0.024	0.045	0.113
7	0.001	0.002	0.009
θ	106.8 ± 19.3	106.3 ± 21.0	105.0 ± 24.3
ρ	0.460	0.467	0.482

nations, average bonding angles θ , and the densities are given. From this data we arrive at an estimate of the melting temperature for the slow heating process of $T_{at} \approx 0.043$ (~ 1082 K), lower than the value obtained by the fast heating. We note however that the first-order character of the transition and the latent heat associated with it are similar to those found before.

IV. CONCLUSIONS

In this paper we have developed a procedure for preparing amorphous silicon using molecular-dynamics simulations and employing the interaction potentials suggested by Stillinger and Weber.¹² In this procedure the system is first prepared at high temperature and then cooled using an increased three-body potential term, thus enhancing the tendency toward tetrahedral coordination. Once the path which the system traverses in its configurational space has been redirected in this manner, restoring the value of the coefficient (λ) of the three-body potential term to its original SW value ($\lambda=21$) results in an amorphous material which exhibits structural, dynamical, and thermodynamical properties in agreement with experimental data. Furthermore, upon fast heating, the so-prepared amorphous silicon melts via a first-order

phase transition at a temperature which is 230 K below the crystalline melting temperature in agreement with experimental measurements. When the behavior of fully relaxed configurations of the amorphous material at several temperatures is analyzed we find that the nature of the transition and the latent heat associated with it maintains, but melting starts at a lower temperature. While a direct cooling of a SW liquid into the amorphous phase, has not yet been achieved,^{16,17} the preparation procedure which we developed demonstrates that it is possible to prepare the amorphous phase using the SW potentials and it can be utilized for studies of the properties of the amorphous phase under various conditions, and in investigations of transformations of the amorphous phase. We are currently investigating additional methods for preparation of amorphous silicon using the SW potential.

ACKNOWLEDGMENTS

This work was supported by U.S. Department of Energy under Grant No. FG05-86ER45234. The computations were performed on the CRAY-XMP at the National Magnetic Fusion Energy Computer Center, Livermore, California.

- ¹*Amorphous Semiconductors*, edited by M. H. Brodsky (Springer, Berlin, 1985).
- ²*Tetrahedrally-Bonded Amorphous Semiconductors*, edited by D. Adler and H. Fritzsche (Plenum, New York, 1985).
- ³*Amorphous Materials: Modeling of Structure and Properties*, Conference Proceedings of the Metallurgical Society of AIME, edited by V. Vitek (AIME, New York, 1983).
- ⁴S. C. Moss, in *Amorphous and Liquid Semiconductors*, edited by J. Stuke and W. Brenig (Taylor and Francis, London, 1974), p. 17.
- ⁵See reviews by G. Lucovsky and T. M. Hayes, in *Amorphous Semiconductors*, Ref. 1, p. 215; M. A. Paesler and D. E. Sayers, in *Tetrahedrally-Bonded Amorphous Semiconductors*, Ref. 2, p. 37.
- ⁶D. E. Polk, *J. Non-Cryst. Solids* **5**, 365 (1971).
- ⁷D. Henderson and F. Herman, *J. Non-Cryst. Solids* **8-10**, 359 (1972); D. Henderson, *J. Non-Cryst. Solids* **16**, 317 (1974).
- ⁸L. Guttman, *Phys. Rev. B* **23**, 1866 (1981).
- ⁹F. Wooten, K. Winer, and D. Weaire, *Phys. Rev. Lett.* **54**, 1392 (1985).
- ¹⁰S. Kirkpatrick, C. D. Gelatt, Jr., and M. P. Vecchi, *Science* **220**, 671 (1983).
- ¹¹See articles in *Computer-Based Microscopic Description of the Structures and Properties of Materials*, Vol. 63 of *Material Research Society Symposium Proceeding*, edited by J. Broughton, W. Krakow, and S. T. Pantelides (MRS, Providence, RI, 1985).
- ¹²F. H. Stillinger and T. A. Weber, *Phys. Rev. B* **31**, 5262 (1985).
- ¹³R. Biswas and D. R. Hamann, *Phys. Rev. Lett.* **55**, 2001 (1985).
- ¹⁴E. Pearson, T. Takai, T. Halicioglu, and W. A. Tiller, *J. Cryst. Growth* **70**, 33 (1984).
- ¹⁵J. Tersoff, *Phys. Rev. Lett.* **56**, 632 (1986).
- ¹⁶J. Q. Broughton and X. P. Li, *Phys. Rev. B* **35**, 9120 (1987).
- ¹⁷K. Ding and H. C. Anderson, *Phys. Rev. B* **34**, 6987 (1986).
- ¹⁸M. D. Kluge, J. R. Ray, and A. Rahman, *J. Chem. Phys.* **85**, 4028 (1986).
- ¹⁹F. F. Abraham and J. P. Batra, *Surf. Sci.* **163**, L752 (1985).
- ²⁰U. Landman, W. D. Luedtke, R. N. Barnett, C. L. Cleveland, M. W. Ribarsky, E. Arnold, S. Ramesh, H. Baumgart, A. Martinez, and B. Khan, *Phys. Rev. Lett.* **56**, 155 (1986).
- ²¹F. F. Abraham and J. Q. Broughton, *Phys. Rev. Lett.* **56**, 734 (1986).
- ²²U. Landman, W. D. Luedtke, M. W. Ribarsky, R. N. Barnett, and C. L. Cleveland, *Phys. Rev. B* (to be published).
- ²³*Physics of Structurally Disordered Solids*, edited by S. S. Mitra (Plenum, New York, 1976). See D. Turnbull, p. 1, and references therein.
- ²⁴M. Parinello and A. Rahman, *Phys. Rev. Lett.* **45**, 1196 (1980).
- ²⁵As seen from Eq. (1c) the three-body terms add a positive contribution to the potential energy, which vanishes for perfect tetrahedral bonding. Thus states with a lower degree of tetrahedral order are characterized by a higher value of V_3 , and may be destabilized by increasing the weight of this term in the potential.
- ²⁶S. C. Moss and J. F. Graczyk, *Phys. Rev. Lett.* **23**, 1167 (1969); see the RDF for amorphous Ge, R. J. Temkins, W. Paul, and G. A. N. Connell, *Adv. Phys.* **22**, 581 (1973).
- ²⁷See reviews in *Semiconductors and Semimetals: Pulsed Laser Processing of Semiconductors*, Proceedings of the National Research Society, edited by R. F. Wood, C. W. White, and R. T. Young (Academic, New York, 1982).
- ²⁸F. Spaepen and D. Turnbull, in *Laser-Solid Interactions and Laser Processing-1978* (Materials Research Society, Boston), Proceedings of the Symposium on Laser-Solid Interactions and Laser Processing, AIP Conf. Proc. No. 50, edited by S.

- D. Ferris, H. J. Leamy, and J. M. Poate (AIP, New York, 1979).
- ²⁹B. G. Bagley and H. S. Chen, in *Laser-Solid Interactions and Laser Processing*, Ref. 28, pg. 97.
- ³⁰E. R. Donovan, F. Spaepen, D. Turnbull, J. M. Poate, and D. C. Jacobson, *J. Appl. Phys.* **57**, 1795 (1985).
- ³¹P. Baeri, G. Foti, J. M. Poate, and A. G. Cullis, *Phys. Rev. Lett.* **45**, 2036 (1980).